

1 Mapping of West Siberian taiga wetland complexes using Landsat 2 imagery: Implications for methane emissions

3 Terentieva I. E.^{1*}, Glagolev M. V.^{1,2,3,4}, Lapshina E. D.², Sabrekov A. F.¹ and
4 Maksyutov S.⁵

5 [1] {Tomsk State University, Tomsk, Russia}

6 [2] {Yugra State University, Khanty-Mansyisk, Russia}

7 [3] {Moscow State University, Moscow, Russia}

8 [4] {Institute of Forest Science, Moscow region, Russia}

9 [5] {National Institute for Environmental Studies, Tsukuba, Japan}

10 [*] {previously published as Kleptsova I. E.}

11 Correspondence to: I. E. Terentieva (kleptsova@gmail.com)

12

13 Abstract

14 High latitude wetlands are important for understanding climate change risks because these
15 environments sink carbon dioxide and emit methane. Fine-scale heterogeneity of wetland
16 landscapes poses a serious challenge when generating regional-scale estimates of greenhouse
17 gas fluxes from point observations. To reduce uncertainties at the regional scale, we mapped
18 wetlands and water bodies in the taiga zone of The West Siberia Lowland (WSL) on a scene-
19 by-scene basis using a supervised classification of Landsat imagery. Training data consists of
20 high-resolution images and extensive field data collected at 28 test areas. The classification
21 scheme aims at supporting methane inventory applications and includes 7 wetland ecosystem
22 types comprising 9 wetland complexes distinguishable at the Landsat resolution. To merge
23 typologies, mean relative areas of wetland ecosystems within each wetland complex type were
24 estimated using high-resolution images. Accuracy assessment based on 1082 validation
25 polygons of 10×10 pixel size indicated an overall map accuracy of 79%. The total area of the
26 WS wetlands and water bodies was estimated to be 52.4 Mha or 4-12% of the global wetland
27 area. Ridge-hollow complexes prevail in WS's taiga zone accounting for 33% of the total
28 wetland area, followed by pine bogs or "ryams" (23%), ridge-hollow-lake complexes (16%),
29 open fens (8%), palsa complexes (7%), open bogs (5%), patterned fens (4%), and swamps (4%).

1 Various oligotrophic environments are dominant among wetland ecosystems, while poor fens
2 cover only 14% of the area. Because of the significant change in the wetland ecosystem
3 coverage in comparison to previous studies, a considerable reevaluation of the total CH₄
4 emissions from the entire region is expected. A new Landsat-based map of WS's taiga wetlands
5 provides a benchmark for validation of coarse-resolution global land cover products and
6 wetland datasets in high latitudes.

7

8 **1 Introduction**

9 High latitude wetlands are important for understanding climate change mechanism as they
10 provide long term storage of carbon and emit significant amount of methane. The West Siberia
11 Lowland (WSL) is the world's largest high-latitude wetland system and experiences an
12 accelerated rate of climate change (Solomon et al., 2007).

13 Poorly constrained estimates of wetland and lake area constitute a major uncertainty in
14 estimating current and future greenhouse gas emissions (Melton et al., 2013; Turetsky et al.,
15 2014; Petrescu et al., 2010). Although wetland extent in WSL has been reasonably well
16 captured by global products based on topographic maps (Lehner and Döll, 2004; Matthews and
17 Fung, 1987), fine-scale heterogeneity of WSL's wetland landscapes (Bohn et al., 2007) requires
18 adding fine scale information in ecosystem functioning as made in wetland CH₄ emission
19 inventory (Glagolev et al., 2011) and estimates of net primary production (Peregon et al., 2008).
20 Present land cover products fail to capture fine-scale spatial variability within WSL's wetlands
21 because of lack of detail necessary for reliable productivity and emissions estimates. Frey and
22 Smith (2007) mentioned insufficient accuracy of four global vegetation and wetland products
23 with the best agreement of only 56% with the high-resolution WSL Peatland Database
24 (WSLPD) (Sheng et al., 2004). Some products (Schroeder et al., 2010; Papa et al., 2010) tend
25 to map only inundation, overlooking areas of «unsaturated» wetlands where the water table is
26 below the moss cover. Because boreal peatlands does not experience prolonged inundation,
27 such products underestimate their area (Krankina et al., 2008). Uncertainty in wetland inventory
28 results in severe biases in CH₄ emission estimates, the scale of differences has been shown by
29 Bohn et al. (2015).

30 Modelers simulating methane emission are in need for high-resolution wetland maps that do
31 not only delineate wetlands but also identify the major sub-types to which different
32 environmental parameters could potentially be applied (Bohn et al., 2015). Several wetland

1 maps have been used to define the wetland extent in WSL, however their application to net
2 primary production (NPP) and methane emission inventories was accompanied by difficulties
3 due to crude classification scheme, limited ground truth data and low spatial resolution. One
4 peatland typology map that distinguishes several vegetation and microtopography classes and
5 their mixtures was developed at the State Hydrological Institute (SHI) by Romanova et al.
6 (1977). Peregon et al. (2005) digitized and complemented this map by estimating the fractional
7 coverage of wetland structural components using Landsat images and aerial photographs for
8 five test sites. However, the limited amount of fractional coverage data and coarse resolution
9 still result in large uncertainties in upscaling methane fluxes (Kleptsova et al., 2012).

10 Our goal was to develop a multi-scale approach for mapping wetlands using Landsat imagery
11 with a resolution of 30 m so the results could better meet the needs of land process modelling
12 and other applications concerning methane emission from peatlands. In this study, the WSL
13 taiga zone was chosen as the primary target for the land cover classification due to wetland
14 abundance. The objectives were: first, to develop a consistent land cover of wetland classes and
15 its structural components; second, to provide the foundation for environmental parameter
16 upscaling (greenhouse gas inventories, carbon balance, NPP, net ecosystem exchange, biomass,
17 etc) and validation of the process models.

18

19 **2 Materials and Methods**

20 **2.1 Study Region**

21 The West Siberian Lowland is a geographical region of Russia bordered by the Ural Mountains
22 in the west and the Yenisey River in the east; the region covers 275 Mha within 62-89°E and
23 53-73°N. Because of its vast expanse and flat terrain, the vegetation cover of the Lowland
24 shows clear latitudinal zonation. According to Gvozdetsky (1968), the taiga zone is divided into
25 three geobotanical subzones: northern taiga, middle taiga and southern taiga. Taiga corresponds
26 to the raised string bog province and covers about 160 Mha in the central part of the WS. It is
27 characterized by flat terrain with elevations of 80 to 100 m above sea level rising to about 190
28 m in the «Siberian Uvaly» area. Average annual precipitation is about 450-500 mm and
29 evaporation is 200-400 mm (National Atlas of Russia, 2008). The excess water supply and flat
30 terrain with poor drainage provides favorable conditions for wetland formation. Comprehensive

1 synthesis of Russian literature regarding the current state of the WSL peatlands, their
2 development and sensitivity to climatic changes was made by Kremenetski et al. (2003).

3 **2.2 Classification methodology**

4 No single classification algorithm can be considered as optimal methodology for improving
5 vegetation mapping; hence, the use of advanced classifier algorithms must be based on their
6 suitability for achieving certain objectives in specific applications (Adam et al., 2009). Because
7 mapping over large areas typically involves many satellite scenes, multi-scene mosaicking is
8 often used to group scenes into a single file set for further classification. This approach
9 optimizes both the classification process and edge matching. However, large multi-scene
10 mosaicking has essential drawback when applying to highly heterogeneous WSL wetlands. It
11 creates a variety of spectral gradients within the file (Homer and Gallant, 2001), especially
12 when the number of the appropriate scenes is limited. It results in spectral discrepancy that is
13 difficult to overcome. In this study, the advantages of consistency in class definition of the
14 scene-by-scene classification approach were considered to outweigh the inherent disadvantages
15 of edge matching and processing labor. Thus, our entire analysis was performed on a scene-by-
16 scene basis, similarly to efforts by Giri et al. (2011) and Gong et al. (2013).

17 For land cover consistency, data of the same year and season, preferably of the growing season
18 peak (July) are required. However, the main complication was the low availability of good
19 quality cloudless images of WSL during those periods. Scenes collected earlier than the 2000s
20 were very few, so they were used as substitutes for places where no other suitable imagery
21 could be found. Landsat-7 images received after 2003 were not used due to data gaps, while
22 Landsat-8 was launched after the starting our mapping procedure. Finally, we collected 70
23 suitable scenes during the peak of the growing seasons in different years. Majority of the images
24 were Landsat 5 TM scenes from July 2007. The scene selection procedure was facilitated by
25 the ability of smoothing the slight inconsistencies between images by specifying training sites
26 in overlapping areas.

27 The overall work flow involves data pre-processing, preparation of the training and test sample
28 collections, image classification on a scene-by-scene basis, regrouping of the derived classes
29 into 9 wetland complexes, the estimation of wetland ecosystem fractional coverage and
30 accuracy assessment. Atmospheric correction was not applied because this process is
31 unnecessary as long as the training data are derived from the image being classified (Song et

1 al., 2001). All of the images were re-projected onto the Albers projection. Because the WSL
2 vegetation includes various types of forests, meadows, burned areas, agricultural fields, etc.,
3 wetland environments were first separated from other landscapes to avoid misclassification. We
4 used thresholds of the Green-Red Vegetation Index (Motohka et al., 2010) to separate majority
5 of wetlands and forests. Thresholds of the 5th Landsat channel (1.55-1.75 μm) was used to
6 mask water bodies and many inundated areas (even vegetated) with the water level up to a few
7 cm below the soil surface. Thresholds were empirically determined for each scene by testing
8 various candidate values. Masked Landsat images were filtered in MATLAB v.7.13
9 (MathWorks) to remove random noise and then classified in Multispec v.3.3 (Purdue Research
10 Foundation) using a supervised classification method. The maximum likelihood algorithm was
11 used because of its robustness and availability in almost any image-processing software (Lu
12 and Weng, 2007). All Landsat bands except the thermal infrared band were used.

13 Training data plays a critical role in the supervised classification technique. Representative data
14 preparation is the most time-consuming and labour-intensive process in regional scale mapping
15 efforts (Gong et al., 2013). As a primary source of information, we used the extensive dataset
16 of botanical descriptions, photos, pH and electrical conductivity data from 28 test sites in WSL
17 (Glagolev et al., 2011). Due to vast expanse and remoteness of WSL, we still had a lack of the
18 ground truth information, which hampered training dataset construction. As a result, we had to
19 rely mostly on high-resolution images available from Google Earth. They came from several
20 satellites (QuickBird, WorldView, GeoEye, IKONOS) with different sensor characteristics;
21 multispectral images were reduced to visible bands (blue, green, red) and had spatial resolution
22 of 1-3 meters. The processing started with mapping scenes where ground truth data and high-
23 resolution images are extensively available, so the classification results could be checked for
24 quality assurance; mapping continued through adjacent images and ended at the less explored
25 scenes with poor ground truth data coverage.

26 To collect training data most efficiently, we used criteria similar to those used by (Gong et al.,
27 2013) for training sample selection: (i) the training samples must be homogeneous; mixed land-
28 cover and heterogeneous areas are avoided; and (ii) all of the samples must be at least 10 pixels
29 in size with an average sample area of approximately 100-200 pixels. The Bhattacharyya
30 distance was used as a class separability measure. The classifier was designed using training
31 samples and then evaluated by classifying input data. The percentage of misclassified samples
32 was taken as an optimistic predication of classification performance (Jain et al., 2000). When

1 accuracy of more than 80% across the training set was attained with no fields showing
2 unreasonable or unexplainable errors, the classification process was started. Classification
3 mismatch between scenes was minimized by placing training samples in overlapping areas.
4 Combining the classified images and area calculations were made using GRASS module in
5 Quantum GIS. Noise filter was applied to eliminate objects smaller than 2×2 pixels. After that,
6 a 10×10-pixel moving window was used to determine the dominant class, which was further
7 assigned to the central 4×4-pixel area.

8 **2.3 Wetland typology development**

9 As a starting point for the mapping procedure, a proper classification scheme is required.
10 Congalton et al. (2014) showed that the classification scheme alone may result in largest error
11 contribution and thus deserves highest implementation priority. Its development should rely on
12 the study purposes and the class separability of the input variables. In our case, wetland
13 mapping was initially conceived as a technique to improve the estimate of the regional CH₄
14 emissions and, secondarily, as a base to upscale other ecological functions. WSL wetlands are
15 highly heterogeneous, however, within each wetland complex we can detect relatively
16 homogeneous structural elements or “wetland ecosystems” with similar water table levels
17 (WTL), geochemical conditions, vegetation covers and, thus, rates of CH₄ emissions (Sabrekov
18 et al., 2013). To ensure a reliable upscaling, we assigned 7 wetland ecosystems in our
19 classification scheme (Fig. 1; Table 1).

20 However, wetland ecosystems generally have sizes from a few to hundreds of meters and cannot
21 be directly distinguished using Landsat imagery with 30-meter resolutions. Therefore, we
22 developed a second wetland typology that involves 9 mixed “wetland complexes” composing
23 wetland ecosystems in different proportions (Fig. 1; Table 2). The classification were adapted
24 from numerous national studies (Katz and Neishtadt, 1963; Romanova, 1985; Liss et al., 2001;
25 Lapshina, 2004; Solomeshch, 2005; Usova, 2009; Masing et al., 2010) and encompassed
26 wooded, patterned, open wetlands and water bodies. The criteria for assigning wetland
27 complexes were: (i) separability on Landsat images, and (ii) abundance in the WSL taiga zone.
28 Each wetland complex represents integral class containing several subtypes differing in
29 vegetation composition and structure. Subtypes were mapped using Landsat images and then
30 generalized into final 9 wetland complexes basing upon ecosystem similarity and spectral
31 separability.

1 To merge typologies, we estimated relative areas of wetland ecosystems within each wetland
2 complex of the final map. Depending on heterogeneity, 8 to 27 test sites of 0.1-1 km² size were
3 selected for each heterogeneous wetland complex. High-resolution images of 1-3 m resolution
4 corresponding to these areas were classified in Multispec v.3.3 using visible channels. An
5 unsupervised ISODATA classification was done on the images specifying 20 classes with a
6 convergence of 95%. Obtained classes were manually reduced to seven wetland ecosystem
7 types. Their relative proportions were calculated and then averaged among the test sites.

8 Thus, we used multiscale approach relying in two typologies. First, typology of wetland
9 complexes was used for mapping Landsat images; second, typology of wetland ecosystems was
10 used for upscaling CH₄ fluxes. The approach is similar to one devised by Peregon et al. (2005),
11 where relative area proportions of “micro-landscape” elements within SHI wetland map were
12 used for NPP data upscaling.

13 During wetland typology development, we made several assumptions. Firstly, the wetland
14 complexes were considered as individual objects, while they actually occupy a continuum with
15 no clustering into discrete units. Secondly, we assumed that all of the wetland water bodies
16 originated during wetland development have sizes less than 2×2 Landsat pixels. They are
17 represented by wetland pools and waterlogged hollows, which are structural components of
18 RHLC. The rest of the water bodies were placed into the “Lakes and rivers” class. Thirdly, in
19 this study, we only consider peatlands and water bodies; floodplain areas were separated from
20 wetlands during the classification process.

21 The concept of wetland ecosystems has merits for CH₄ emission inventory. Methane emission
22 depends mainly on water table level, temperature, and trophic state (Dise et al., 1993; Dunfield
23 et al., 1993; Conrad, 1996). We take into consideration temperature, when we upscale fluxes
24 separately for southern, middle and northern taiga. We take into consideration trophic state,
25 when we map wetland complexes using multispectral Landsat images. We take into
26 consideration water table level, when we map vegetation of wetland ecosystems with high-
27 resolution images, because vegetation reflects soil moisture conditions. We do not directly
28 consider smallest spatial elements as hummocks and tussocks. This omission introduces some
29 uncertainty in regional CH₄ emission estimate, which was evaluated by (Sabrekov et al., 2014).
30 Accordingly, reliable estimate of CH₄ fluxes accounting for fine spatial detail requires large
31 number of measurements. Such heterogeneity is being addressed by measuring fluxes in all
32 microforms in the field and then obtaining probability density distributions.

1

2 **3 Results and Discussion**

3 **3.1 Wetland map**

4 Based on Landsat imagery, we developed a high-resolution wetland inventory of the WSL taiga
5 zone (Fig. 2). The total area of wetlands and water bodies was estimated to be 52.4 Mha. West
6 Siberian taiga wetlands are noticeable even from global prospective. The global total of
7 inundated areas and peatlands was estimated to cover from 430 (Cogley, 1994) to 1170 Mha
8 (Lehner and Döll, 2004) as summarized by Melton et al. (2013); therefore, taiga wetlands in
9 WSL account for approximately from 4 to 12% of the global wetland area. Their area is larger
10 than the wetland areas of 32.4, 32, and 41 Mha in China (Niu et al., 2012), Hudson Bay Lowland
11 (Cowell, 1982) and Alaska (Whitcomb et al., 2009), respectively. The extent of West Siberia's
12 wetlands exceeds the tropical wetland area of 43.9 Mha (Page et al., 2011) emphasizing the
13 considerable ecological role of the studied region.

14 As summarized by Sheng et al. (2004), the majority of earlier Russian studies estimated the
15 extent of the entire WS's mires to be considerably lower. These studies probably inherited the
16 drawbacks of the original Russian Federation Geological Survey database, which was used as
17 the basis for the existing WSL peatland inventories (Ivanova and Novikova, 1976). This
18 database suffered from lack of field survey data in remote regions, a high generalization level
19 and only considered economically valuable peatlands with peat layers deeper than 50 cm.

20 Our peatland coverage is similar to the estimate of 51.5 Mha (Peregon et al., 2009) by SHI map
21 (Romanova et al., 1977). However, a direct comparison between the peatland maps shows that
22 the SHI map is missing important details on the wetland distribution (Fig. 3). SHI map was
23 based on aerial photography, which was not technically viable for full and continuous mapping
24 of a whole region because it is too costly and time-consuming to process (Adam et al., 2009).

25 Distribution of wetland ecosystem areas have changed significantly in comparison to SHI map
26 (Peregon et al., 2009); in particular, we obtained 105% increase in spatial extent of CH₄ high-
27 emitting ecosystems such as waterlogged, oligotrophic hollows and fens. In the case study of
28 WS's middle taiga, we found that applying the new wetland map led to a 130% increase in the
29 CH₄ flux estimate from the domain (Kleptsova et al., 2012) in comparison with the estimate
30 based on SHI map. Thus, a considerable revaluation of the total CH₄ emissions from the whole
31 region is expected.

1 **3.2 Regularities of zonal distribution**

2 WS has a large variety of wetlands that developed under different climatic and geomorphologic
3 conditions. Concerning the wetland complex typology (excluding “Lakes and rivers” class),
4 RHCs prevail in WS’s taiga, accounting for 32.2% of the total wetland area, followed by pine
5 bogs (23%), RHLCs (16.4%), open fens (8.4%), palsa complexes (7.6%), open bogs (4.8%),
6 patterned fens (3.9%) and swamps (3.7%). Various bogs are dominant among the wetland
7 ecosystems (Table 3), while fens cover only 14.3% of the wetlands. Waterlogged hollows and
8 open water occupy 7% of the region, which is similar to the estimate by Watts et al. (2014),
9 who found that 5% of the boreal-Arctic domain was inundated during summer season.

10 The individual wetland environments have a strongly pronounced latitudinal zonality within
11 the studied region. Zonal borders stretch closely along latitude lines, subdividing the taiga
12 domain into the southern, middle, and northern taiga subzones (Fig. 2, black lines). To visualize
13 the regularities of the wetland distribution, we divided the entire area into $0.1^{\circ} \times 0.1^{\circ}$ grids and
14 calculated ratios of wetland ecosystem areas to the total cell areas for each grid (Fig. 4) using
15 fractional coverage data from Table 2.

16 Mire coverage of WSL’s northern taiga ($62-65^{\circ}\text{N}$) is approximately 36%. Because of the
17 abundance of precipitation, low evaporation and slow runoff, the northern taiga is characterized
18 by largest relative area of lakes and waterlogged hollows, covering a third of the domain (Fig.
19 4a, b). Vast parts of the zone are occupied by the peatland system “Surgutskoe Polesye,” which
20 stretches for one hundred kilometers from east to west between 61.5°N and 63°N . Peatland and
21 water bodies cover up to 70% of the territory, forming several huge peatland-lake complexes
22 divided by river valleys. Northward, the slightly paludified “Sibirskie Uvaly” elevation
23 (63.5°N) divides the northern taiga into two lowland parts. Palsa hillocks appear in the
24 “Surgutskoe Polesye” region and replace the ridges and ryams to the north of the “Sibirskie
25 Uvaly” region (Fig. 4f).

26 RHCs are the most abundant in the middle taiga ($59-62^{\circ}\text{N}$), where mires occupy 34% of the
27 area. Large wetland systems commonly cover watersheds and have a convex dome with centres
28 of 3-6 m higher than periphery. These environments have peat layer of several meters depth
29 composed of sphagnum peat with the small addition of other plants. The wetland ecosystems
30 here have distinct spatial regularities. Central plateau depressions with stagnant water are
31 covered by RHLCs. Different types of RHCs cover better-drained gentle slopes. The most

1 drained areas are dominated by ryams. Poor and rich fens develop along wetland's edges with
2 relatively high nutrient availability. Wooded swamps usually surround vast wetland systems.
3 The wetland extent reaches 28% in WS's southern taiga area (56-59°N). Wetlands are
4 composed of raised bogs alternating with huge open and patterned fens. The eastern part of the
5 subzone is dominated by small and medium-sized wetland complexes. The southern and middle
6 taiga wetlands exhibit similar spatial patterns; however, the area of fens increases southwards
7 due to the abundance of carbonate soils and higher nutrient availability. Velichko et al. (2011)
8 provide evidence for existence of a vast cold desert in the northern half of the WSL at the late
9 glacial time, whereas the southernmost part was an area of loess accumulation. The border
10 between fen and bog-dominated areas extends near 59°N and corresponds to the border between
11 the southern and middle taiga zones (Fig. 4c and e).

12 **3.3 Accuracy assessment**

13 The map accuracy assessment was based on 1082 validation polygons of 10×10 pixels that were
14 randomly spread over the WSL taiga zone. We used high-resolution images available in Google
15 Earth as the ground truth information. The confusion matrix (Table 4) was used as a way to
16 represent map accuracy (Congalton and Green, 2008). Overall, we achieved the classification
17 accuracy of 79% that can be considered reasonable for such a large and remote area. We found
18 that the accuracies for different land-cover categories varied from 62 to 99%, with the lake and
19 river, ryam, and RHC class areas mapped most successfully and open bogs and patterned fens
20 being the most confused. Some errors were associated with mixed pixels (33 polygons), whose
21 presence had been recognized by Foody (2002) as a major problem, affecting the effective use
22 of remotely sensed data in per-pixel classification.

23 Wetland complexes within large wetland systems had the highest classification accuracies. In
24 contrast, the uncertainties are particularly high for small objects. It is of special importance in
25 southern part of the domain, where highly heterogeneous agricultural landscapes neighbour
26 upon numerous individual wetlands of 100-1000 ha area. Several vegetation indices was tested
27 to map them; however, the best thresholding result was achieved by using Landsat thermal
28 band. In addition, many errors happened along the tundra boundary caused by the lack of
29 ground truth data combined with the high landscape heterogeneity. However, those small areas
30 mainly correspond to palsa complexes and have slight impact on CH₄ flux estimate.

1 Misclassifications usually occurred between similar classes introducing only a minor distortion
2 in map applications. Patterned fens and open bogs were classified with the lowest producer's
3 accuracy (PA) of 62%. Patterned fens include substantial treeless areas, so they were often
4 misclassified as open fens. They were also confused with RHCs due to the similar "ridge-
5 hollow" structure. Some open bogs have tussock shrub cover with sparsely distributed pine
6 trees provoking misclassification as RHCs and pine bogs. Open fens have higher user's
7 accuracy (UA) and PA; however, visible channels of high-resolution images poorly reflect
8 trophic state, which underrates classification errors between open bogs and open fens. Swamps
9 and palsa complexes have very high PA and low UA, which is related to their incorrect
10 identification in non-wetland areas. Palsa complexes were spectrally close to open woodlands
11 with lichen layer, which covers wide areas of WSL north taiga. During dry period, swamps
12 were often confused with forests, whereas in the field they can be easily identified through the
13 presence of peat layers and a characteristic microrelief. In both cases, more accurate wetland
14 masks would lead to substantially higher accuracy levels. Lakes and rivers were classified the
15 best due to the high spectral separability of the class. They can be confused with RHLCs
16 represented by a series of small lakes or waterlogged hollows alternating with narrow
17 isthmuses. Floodplains after snow melt can also be classified as lakes (11 polygons). RHCs and
18 pine bogs were accurately identified due to their abundance in the study region and high spectral
19 separability.

20 **3.4 Challenges and future prospects**

21 The contrast between vast wetland systems and the surrounding forests is so distinct in WSL
22 that wetlands can be adequately identified by the summer season images (Sheng et al., 2004).
23 On the contrary, correct mapping of wetland with pronounced seasonal variations remains one
24 of the largest challenges. Wetlands become the most inundated after snow melt or rainy periods
25 resulting in partial transformation of oligotrophic hollows and fens into waterlogged hollows
26 (see hollows with brown Sphagnum cover at Fig. 1). Image features of swamps after drought
27 periods become similar to forests. Interannual variability of water table level in WSL wetlands
28 (Schroeder et al., 2010; Watts et al., 2014) also makes impact on mapping results.

29 New methodologies and protocols are needed to improve our ability to monitor water levels
30 (Kim et al., 2009). Observations of soil moisture and wetland dynamic using radar data such as
31 PALSAR (Chapman et al., 2015; Clewley et al., 2015) and Global Navigation Satellite Signals
32 Reflectometry are promising (Chew et al., 2016; Zuffada et al., 2015). Advanced classification

1 techniques such as fuzzy logic can be applied for mapping fine-scale heterogeneity (Adam et
2 al., 2009). Recent innovations in wetland mapping were described by Tiner et al. (2015).

3 Water table fluctuations are especially important for upscaling CH₄ fluxes because the spatial
4 distribution of methane emissions, and therefore, the total methane emission, are functions of
5 the spatial distribution of water table depths (Bohn et al., 2007). Wetland ecosystems with water
6 levels close to surface contribute most to the regional flux, while the contribution of dryer
7 ecosystems (ryams, ridges and palsa hillocks) is close to negligible (Glagolev et al., 2011;
8 Sabrekov et al., 2014).

9 Although the synergistic combination of active and passive microwave sensor data is
10 advantageous for accurately characterizing open water (Schroeder et al., 2010) and wetlands,
11 the remote sensing of water regimes is successful only when in situ data are available for
12 calibration. We still lack in situ measurements of the water table dynamics within WSL
13 wetlands. Limited monitoring have been made at the Bakchar field station (Krasnov et al., 2013;
14 Krasnov et al., 2015) and Mukhrino field station (Bleuten and Filippov, 2008); however, the
15 vast majority of obtained data are not yet analyzed and published. These measurements are of
16 special importance for the northern taiga and tundra, where shallow thermokarst lakes with
17 fluctuating water regimes cover huge areas.

18 The scarcity of reliable reference data and subsequent lack of consistency also limit the
19 accuracy of maps (Homer and Gallant, 2001). The use of ancillary data can largely improve it
20 (Congalton et al., 2014); however, more reliable classification accuracy comes with significant
21 costs regarding detailed field data. The next step in map improvement should rely on the
22 acquisition of more ground truth data for the poorly classified wetland types and remote regions.
23

24 **4 Conclusions**

25 Boreal peatlands play a major role in carbon storage, methane emissions, water cycling and
26 other global environmental processes, but better understanding of this role is constrained by the
27 inconsistent representation of peatlands on (or even complete omission from) many global land
28 cover maps (Krankina et al., 2008). In this study, we developed a map representing the state of
29 the taiga wetlands in WSL during the peak of the growing season. The efforts reported here can
30 be considered as an initial attempt at mapping boreal wetlands using Landsat imagery, with the
31 general goal of supporting the monitoring of wetland resources and upscaling the methane

1 emissions from wetlands and inland waters. The resulting quantitative definitions of wetland
2 complexes combined with a new wetland map can be used for the estimation and spatial
3 extrapolation of many ecosystem functions from site-level observations to the regional scale.
4 In the case study of WS's middle taiga, we found that applying the new wetland map led to a
5 130% increase in the CH₄ flux estimation from the domain (Kleptsova et al., 2012) comparing
6 with estimation based on previously used SHI map. Thus, a considerable reevaluation of the
7 total CH₄ emissions from the entire region is expected.

8 We estimate a map accuracy of 79% for this large and remote area. The next step in improving
9 mapping quality will depend on the acquisition of ground truth data from the least discernible
10 wetland landscapes and remote regions. Correctly distinguishing wetland complexes with
11 strongly pronounced seasonal variability in their water regimes remains one of the largest
12 challenges. This difficulty can be resolved by installing water level gauge network and usage
13 both combined remote sensing data and advanced classification techniques.

14 Our new Landsat-based map of WS's taiga wetlands can be used as a benchmark dataset for
15 validation of coarse-resolution global land cover products and for assessment of global model
16 performance in high latitudes. Although classification scheme was directed towards improving
17 CH₄ inventory, the resulting map can also be applied for upscaling of the other environmental
18 parameters.

19

20 **Acknowledgements**

21 We thank Amber Soja and anonymous reviewers for assisting in improving the initial version
22 of the manuscript. This study (research grant No 8.1.94.2015) was supported by The Tomsk
23 State University Academic D.I. Mendeleev Fund Program in 2014-2015. The study was also
24 supported by the GRENE-Arctic project by MEXT Japan.

25

26 **References**

27 Adam, E., Mutanga, O., and Rugege, D.: Multispectral and hyperspectral remote sensing for
28 identification and mapping of wetland vegetation: a review, *Wetlands Ecology and*
29 *Management*, 18, 281-296, 10.1007/s11273-009-9169-z, 2009.

1 Bleuten, W., and Filippov, I.: Hydrology of mire ecosystems in central West Siberia: the
2 Mukhrino Field Station, Transactions of UNESCO department of Yugorsky State University
3 “Dynamics of environment and global climate change”/Glagolev MV, Lapshina ED (eds.).
4 Novosibirsk: NSU, 208-224, 2008.

5 Bohn, T. J., Lettenmaier, D. P., Sathulur, K., Bowling, L. C., Podest, E., McDonald, K. C., and
6 Friborg, T.: Methane emissions from western Siberian wetlands: heterogeneity and sensitivity
7 to climate change, *Environmental Research Letters*, 2, 045015, 10.1088/1748-9326/2/4/045015,
8 2007.

9 Bohn, T. J., Melton, J. R., Ito, A., Kleinen, T., Spahni, R., Stocker, B. D., Zhang, B., Zhu, X.,
10 Schroeder, R., Glagolev, M. V., Maksyutov, S., Brovkin, V., Chen, G., Denisov, S. N., Eliseev,
11 A. V., Gallego-Sala, A., McDonald, K. C., Rawlins, M. A., Riley, W. J., Subin, Z. M., Tian, H.,
12 Zhuang, Q., and Kaplan, J. O.: WETCHIMP-WSL: intercomparison of wetland methane
13 emissions models over West Siberia, *Biogeosciences*, 12, 3321-3349, 10.5194/bg-12-3321-
14 2015, 2015.

15 Chapman, B., McDonald, K., Shimada, M., Rosenqvist, A., Schroeder, R., and Hess, L.:
16 Mapping regional inundation with spaceborne L-band SAR, *Remote Sensing*, 7, 5440-5470,
17 2015.

18 Chew, C., Shah, R., Zuffada, C., Hajj, G., Masters, D., and Mannucci, A. J.: Demonstrating soil
19 moisture remote sensing with observations from the UK TechDemoSat - 1 satellite mission,
20 *Geophysical Research Letters*, 43, 3317-3324, 2016.

21 Clewley, D., Whitcomb, J., Moghaddam, M., McDonald, K., Chapman, B., and Bunting, P.:
22 Evaluation of ALOS PALSAR data for high-resolution mapping of vegetated wetlands in
23 Alaska, *Remote Sensing*, 7, 7272-7297, 2015.

24 Cogley, J.: GGHYDRO: global hydrographic data, Peterborough, Ontario, Canada, 1994.

1 Congalton, R., Gu, J., Yadav, K., Thenkabail, P., and Ozdogan, M.: Global Land Cover
2 Mapping: A Review and Uncertainty Analysis, *Remote Sensing*, 6, 12070-12093,
3 10.3390/rs61212070, 2014.

4 Congalton, R. G., and Green, K.: Assessing the accuracy of remotely sensed data: principles
5 and practices, CRC press, Florida, USA, 2008.

6 Conrad, R.: Soil microorganisms as controllers of atmospheric trace gases (H₂, CO, CH₄, OCS,
7 N₂O, and NO), *Microbiological reviews*, 60, 609-640, 1996.

8 Cowell, D. W.: Earth Sciences of the Hudson Bay Lowland: Literature Review and Annotated
9 Bibliography, Lands Directorate, Environment Canada, 1982.

10 Dise, N. B., Gorham, E., and Verry, E. S.: Environmental factors controlling methane emissions
11 from peatlands in northern Minnesota, *Journal of Geophysical Research: Atmospheres* (1984–
12 2012), 98, 10583-10594, 1993.

13 Dunfield, P., Dumont, R., and Moore, T. R.: Methane production and consumption in temperate
14 and subarctic peat soils: response to temperature and pH, *Soil Biology and Biochemistry*, 25,
15 321-326, 1993.

16 Foody, G. M.: Status of land cover classification accuracy assessment, *Remote sensing of*
17 *environment*, 80, 185-201, 2002.

18 Frey, K. E., and Smith, L. C.: How well do we know northern land cover? Comparison of four
19 global vegetation and wetland products with a new ground-truth database for West Siberia,
20 *Global Biogeochemical Cycles*, 21, 10.1029/2006gb002706, 2007.

21 Giri, C., Ochieng, E., Tieszen, L. L., Zhu, Z., Singh, A., Loveland, T., Masek, J., and Duke, N.:
22 Status and distribution of mangrove forests of the world using earth observation satellite data,
23 *Global Ecology and Biogeography*, 20, 154-159, 10.1111/j.1466-8238.2010.00584.x, 2011.

1 Glagolev, M., Kleptsova, I., Filippov, I., Maksyutov, S., and Machida, T.: Regional methane
2 emission from West Siberia mire landscapes, *Environmental Research Letters*, 6, 045214,
3 10.1088/1748-9326/6/4/045214, 2011.

4 Gong, P., Wang, J., Yu, L., Zhao, Y., Zhao, Y., Liang, L., Niu, Z., Huang, X., Fu, H., Liu, S.,
5 Li, C., Li, X., Fu, W., Liu, C., Xu, Y., Wang, X., Cheng, Q., Hu, L., Yao, W., Zhang, H., Zhu,
6 P., Zhao, Z., Zhang, H., Zheng, Y., Ji, L., Zhang, Y., Chen, H., Yan, A., Guo, J., Yu, L., Wang,
7 L., Liu, X., Shi, T., Zhu, M., Chen, Y., Yang, G., Tang, P., Xu, B., Giri, C., Clinton, N., Zhu,
8 Z., Chen, J., and Chen, J.: Finer resolution observation and monitoring of global land cover:
9 first mapping results with Landsat TM and ETM+ data, *International Journal of Remote*
10 *Sensing*, 34, 2607-2654, 10.1080/01431161.2012.748992, 2013.

11 Gvozdetsky, N.: *Physiographic zoning of USSR*, MSU, Moscow, Russia, 576 pp., 1968.

12 Homer, C., and Gallant, A.: Partitioning the conterminous United States into mapping zones
13 for Landsat TM land cover mapping, Unpublished US Geologic Survey report, 2001.

14 Ivanova, K., and Novikova, S.: *West Siberian peatlands, their structure and hydrological regime*,
15 *Gidrometeoizdat*, Leningrad, USSR, 448 pp., 1976.

16 Jain, A. K., Duin, R. P., and Mao, J.: Statistical pattern recognition: A review, *Pattern Analysis*
17 *and Machine Intelligence*, *IEEE Transactions on*, 22, 4-37, 2000.

18 Katz, N., and Neishtadt, M.: Peatlands, in: *West Siberia*, edited by: Rihter, G. D., AS USSR,
19 Moscow, Russia, 230-248, 1963.

20 Kim, J.-W., Lu, Z., Lee, H., Shum, C. K., Swarzenski, C. M., Doyle, T. W., and Baek, S.-H.:
21 Integrated analysis of PALSAR/Radarsat-1 InSAR and ENVISAT altimeter data for mapping
22 of absolute water level changes in Louisiana wetlands, *Remote Sensing of Environment*, 113,
23 2356-2365, 10.1016/j.rse.2009.06.014, 2009.

24 Kleptsova, I., Glagolev, M., Lapshina, E., and Maksyutov, S.: Landcover classification of the
25 Great Vasyugan mire for estimation of methane emission, in: 1st International Conference on

1 “Global Warming and the Human-Nature Dimension in Siberia: Social Adaptation to the
2 Changes of the Terrestrial Ecosystem, with an Emphasis on Water Environments” (7-9 March
3 2012, Kyoto, Japan), 2012.

4 Krankina, O., Pflugmacher, D., Friedl, M., Cohen, W., Nelson, P., and Baccini, A.: Meeting the
5 challenge of mapping peatlands with remotely sensed data, *Biogeosciences*, 5, 1809-1820, 2008.

6 Krasnov, O. A., Maksyutov, S. S., Glagolev, M. V., Kataev, M. Y., Inoue, G., Nadeev, A. I.,
7 and Schelevoi, V. D.: Automated complex “Flux-NIES” for measurement of methane and
8 carbon dioxide fluxes, *Atmospheric and oceanic optics*, 26, 1090-1097, 2013.

9 Krasnov, O. A., Maksyutov, S. S., Davydov, D. K., Fofonov, A. V., and Glagolev, M. V.:
10 Measurements of methane and carbon dioxide fluxes on the Bakchar bog in warm season, *Proc.*
11 *SPIE 9680, 21st International Symposium Atmospheric and Ocean Optics: Atmospheric*
12 *Physics*, 968066 (November 19, 2015), 10.1117/12.2205557, 2015.

13 Kremenetski, K. V., Velichko, A. A., Borisova, O. K., MacDonald, G. M., Smith, L. C., Frey,
14 K. E., and Orlova, L. A.: Peatlands of the Western Siberian lowlands: current knowledge on
15 zonation, carbon content and Late Quaternary history, *Quaternary Science Reviews*, 22, 703-
16 723, 10.1016/s0277-3791(02)00196-8, 2003.

17 Lapshina, E.: Peatland vegetation of south-east West Siberia, TSU, Tomsk, Russia, 296 pp.,
18 2004.

19 Lehner, B., and Döll, P.: Development and validation of a global database of lakes, reservoirs
20 and wetlands, *Journal of Hydrology*, 296, 1-22, 10.1016/j.jhydrol.2004.03.028, 2004.

21 Liss, O., Abramova, L., Avetov, N., Berezina, N., Inisheva, L., Kurnishkova, T., Sluka, Z.,
22 Tolpysheva, T., and Shvedchikova, N.: Mire systems of West Siberia and its nature
23 conservation importance, Grif and Co, Tula, Russia, 584 pp., 2001.

1 Lu, D., and Weng, Q.: A survey of image classification methods and techniques for improving
2 classification performance, *International Journal of Remote Sensing*, 28, 823-870,
3 10.1080/01431160600746456, 2007.

4 Masing, V., Botch, M., and Läänelaid, A.: Mires of the former Soviet Union, *Wetlands ecology
5 and management*, 18, 397-433, 2010.

6 Matthews, E., and Fung, I.: Methane emission from natural wetlands: Global distribution, area,
7 and environmental characteristics of sources, *Global biogeochemical cycles*, 1, 61-86, 1987.

8 Melton, J. R., Wania, R., Hodson, E. L., Poulter, B., Ringeval, B., Spahni, R., Bohn, T., Avis,
9 C. A., Beerling, D. J., Chen, G., Eliseev, A. V., Denisov, S. N., Hopcroft, P. O., Lettenmaier,
10 D. P., Riley, W. J., Singarayer, J. S., Subin, Z. M., Tian, H., Zürcher, S., Brovkin, V., van
11 Bodegom, P. M., Kleinen, T., Yu, Z. C., and Kaplan, J. O.: Present state of global wetland
12 extent and wetland methane modelling: conclusions from a model inter-comparison project
13 (WETCHIMP), *Biogeosciences*, 10, 753-788, 10.5194/bg-10-753-2013, 2013.

14 Motohka, T., Nasahara, K. N., Oguma, H., and Tsuchida, S.: Applicability of green-red
15 vegetation index for remote sensing of vegetation phenology, *Remote Sensing*, 2, 2369-2387,
16 2010.

17 National Atlas of Russia, C. (2008). "Environment (Nature). Ecology": [http://xn--
18 80aaaa1bhncclcci1cl5c4ep.xn--plai/cd2/english.html](http://xn--80aaaa1bhncclcci1cl5c4ep.xn--plai/cd2/english.html), last access: 28 March 2016. In

19 Niu, Z., Zhang, H., Wang, X., Yao, W., Zhou, D., Zhao, K., Zhao, H., Li, N., Huang, H., Li, C.,
20 Yang, J., Liu, C., Liu, S., Wang, L., Li, Z., Yang, Z., Qiao, F., Zheng, Y., Chen, Y., Sheng, Y.,
21 Gao, X., Zhu, W., Wang, W., Wang, H., Weng, Y., Zhuang, D., Liu, J., Luo, Z., Cheng, X.,
22 Guo, Z., and Gong, P.: Mapping wetland changes in China between 1978 and 2008, *Chinese
23 Science Bulletin*, 57, 2813-2823, 10.1007/s11434-012-5093-3, 2012.

24 Page, S. E., Rieley, J. O., and Banks, C. J.: Global and regional importance of the tropical
25 peatland carbon pool, *Global Change Biology*, 17, 798-818, 2011.

1 Papa, F., Prigent, C., Aires, F., Jimenez, C., Rossow, W. B., and Matthews, E.: Interannual
2 variability of surface water extent at the global scale, 1993–2004, *Journal of Geophysical*
3 *Research*, 115, 10.1029/2009jd012674, 2010.

4 Peregon, A., Maksyutov, S., Kosykh, N., Mironycheva-Tokareva, N., Tamura, M., and Inoue,
5 G.: Application of the multi-scale remote sensing and GIS to mapping net primary production
6 in west Siberian wetlands, *Phyton*, 45, 543-550, 2005.

7 Peregon, A., Maksyutov, S., Kosykh, N. P., and Mironycheva - Tokareva, N. P.: Map - based
8 inventory of wetland biomass and net primary production in western Siberia, *Journal of*
9 *Geophysical Research: Biogeosciences (2005–2012)*, 113, 2008.

10 Peregon, A., Maksyutov, S., and Yamagata, Y.: An image-based inventory of the spatial
11 structure of West Siberian wetlands, *Environmental Research Letters*, 4, 045014, 2009.

12 Petrescu, A. M. R., van Beek, L. P. H., van Huissteden, J., Prigent, C., Sachs, T., Corradi, C. A.
13 R., Parmentier, F. J. W., and Dolman, A. J.: Modeling regional to global CH₄ emissions of
14 boreal and arctic wetlands, *Global Biogeochemical Cycles*, 24, 10.1029/2009gb003610, 2010.

15 Romanova, E., Bybina, R., Golitsyna, E., Ivanova, G., Usova, L., and Trushnikova, L.: Wetland
16 typology map of West Siberian lowland scale 1:2500000 GUGK, Leningrad, Russia, 1977.

17 Romanova, E.: Vegetation cover of West Siberian Lowland, in: *Peatland vegetation*, edited by:
18 Il'ina, I., Lapshina, E., Lavrenko, N., Meltser, L., Romanova, E., Bogoyavlenskiy, M., and
19 Mahno, V., Science, Novosibirsk, Russia, 138-160, 1985.

20 Sabrekov, A., Glagolev, M., Kleptsova, I., Machida, T., and Maksyutov, S.: Methane emission
21 from mires of the West Siberian taiga, *Eurasian Soil Science*, 46, 1182-1193, 2013.

22 Sabrekov, A. F., Runkle, B. R. K., Glagolev, M. V., Kleptsova, I. E., and Maksyutov, S. S.:
23 Seasonal variability as a source of uncertainty in the West Siberian regional CH₄ flux upscaling,
24 *Environmental Research Letters*, 9, 045008, 10.1088/1748-9326/9/4/045008, 2014.

1 Schroeder, R., Rawlins, M. A., McDonald, K. C., Podest, E., Zimmermann, R., and Kueppers,
2 M.: Satellite microwave remote sensing of North Eurasian inundation dynamics: development
3 of coarse-resolution products and comparison with high-resolution synthetic aperture radar data,
4 *Environmental Research Letters*, 5, 015003, 10.1088/1748-9326/5/1/015003, 2010.

5 Sheng, Y., Smith, L. C., MacDonald, G. M., Kremenetski, K. V., Frey, K. E., Velichko, A. A.,
6 Lee, M., Beilman, D. W., and Dubinin, P.: A high-resolution GIS-based inventory of the west
7 Siberian peat carbon pool, *Global Biogeochemical Cycles*, 18, 10.1029/2003gb002190, 2004.

8 Solomeshch, A.: *The West Siberian Lowland, The world's largest wetlands: ecology and*
9 *conservation*. Cambridge University Press, Cambridge, 11-62, 2005.

10 Solomon, S., Dahe, Q., Martin, M., Melinda, M., Kristen, A., Melinda M.B. , T., Henry, L. M.,
11 and Zhenlin, C.: *Climate change 2007-the physical science basis: Working group I contribution*
12 *to the fourth assessment report of the IPCC*, Cambridge University Press, 2007.

13 Song, C., Woodcock, C. E., Seto, K. C., Lenney, M. P., and Macomber, S. A.: Classification
14 and change detection using Landsat TM data: when and how to correct atmospheric effects?,
15 *Remote sensing of Environment*, 75, 230-244, 2001.

16 Tiner, R. W., Lang, M. W., and Klemas, V. V.: *Remote Sensing of Wetlands: Applications and*
17 *Advances*, CRC Press, 2015.

18 Turetsky, M. R., Kotowska, A., Bubier, J., Dise, N. B., Crill, P., Hornibrook, E. R., Minkinen,
19 K., Moore, T. R., Myers-Smith, I. H., Nykanen, H., Olefeldt, D., Rinne, J., Saarnio, S., Shurpali,
20 N., Tuittila, E. S., Waddington, J. M., White, J. R., Wickland, K. P., and Wilmking, M.: A
21 synthesis of methane emissions from 71 northern, temperate, and subtropical wetlands, *Glob*
22 *Chang Biol*, 20, 2183-2197, 10.1111/gcb.12580, 2014.

23 Usova, L.: *Aerial photography classification of different West Siberian mire landscapes,*
24 *Nestor-History, Saint-Petersburg*, 83 pp., 2009.

- 1 Watts, J. D., Kimball, J. S., Bartsch, A., and McDonald, K. C.: Surface water inundation in the
2 boreal-Arctic: potential impacts on regional methane emissions, *Environmental Research*
3 *Letters*, 9, 075001, 10.1088/1748-9326/9/7/075001, 2014.
- 4 Whitcomb, J., Moghaddam, M., McDonald, K., Kellndorfer, J., and Podest, E.: Mapping
5 vegetated wetlands of Alaska using L-band radar satellite imagery, *Canadian Journal of Remote*
6 *Sensing*, 35, 54-72, 2009.
- 7 Zuffada, C., Li, Z., Nghiem, S. V., Lowe, S., Shah, R., Clarizia, M. P., and Cardellach, E. (2015).
8 The rise of GNSS reflectometry for Earth remote sensing. In, *Geoscience and Remote Sensing*
9 *Symposium (IGARSS), 2015 IEEE International* (pp. 5111-5114): IEEE

1 Table 1. Wetland ecosystem types

Wetland ecosystem	Short description	WTL, cm (1st/2nd/3rd quartiles)¹
Open water	All water bodies greater than 2×2 Landsat pixels	-
Waterlogged hollows	Open water bodies fewer than 2×2 Landsat pixels or depressed parts of wetland complexes with WTLs above the average moss/vegetation surface	-10 / -7 / -4
Oligotrophic hollows	Depressed parts of bogs with WTLs beneath the average moss/vegetation cover	3 / 5 / 10
Ridges	Long and narrow elevated parts of wetland complexes with dwarf shrubs-sphagnum vegetation cover	20 / 32 / 45
Ryams	Extensive pine-dwarf shrubs-sphagnum areas	23 / 38 / 45
Fens	Integrated class for various types of rich fens, poor fens and wooded swamps	7 / 10 / 20
Palsa hillocks	Elevated parts of palsa complexes with permafrost below the surface	Less than 45

2 ¹ Positive WTL means that water is below average moss/soil surface; the data was taken from field dataset
3 (Glagolev et al., 2011)

4

- 1 Table 2. Wetland types and fractional coverage of wetland ecosystems (Open water – W,
 2 Waterlogged hollows – WH, Oligotrophic hollows – OH, Ridges – R, Ryams – Ry, Fens – F,
 3 Palsa hillocks – P)

Wetland complexes	Short description	Wetland ecosystems
<i>Wooded wetlands</i>		
Pine-dwarf shrubs-sphagnum bogs (pine bogs, ryams)	Dwarf shrubs-sphagnum communities with pine trees (local name – “ryams”) occupy the most drained parts of wetlands. Pine height and crown density are positively correlated with the slope angle. Ryams purely depend on precipitation and the atmospheric input of nutrients. The next evolutionary type under increased precipitation is RHC.	Ry: 100%
Wooded swamps	Wooded swamps develop in areas with close occurrence of groundwater. They frequently surround wetland systems; they can also be found in river valleys and terraces. Wooded swamps are extremely diverse in floristic composition and have prominent microtopography.	F: 100%
<i>Patterned wetlands</i>		
Ridge-hollow complexes (RHC)	RHC consists of alternating long narrow ridges and oligotrophic hollows. They purely depend on precipitation and the atmospheric input of nutrients. The configuration of ridges and hollows depend on the slope angle and hydrological conditions of the contiguous areas. RHCs with small, medium, and large hollows can be arranged within the class.	R: 42% OH: 58%
Ridge-hollow-lake complexes (RHLC)	RHLCs develop on poorly drained watersheds or after seasonal flooding of patterned wetlands. RHLCs are the most abundant in northern taiga. They may include numerous shallow pools. Hollows can be both oligotrophic and meso- or eutrophic.	R: 31% OH: 25% WH: 31% F: 13%
Patterned fens	Patterned fens are widely distributed within the region. They correspond to the WSL type of aapa mires. Patterned fens are composed of meso- or eutrophic hollows alternating with narrow ridges. The vegetation cover commonly includes sedge-moss communities.	R: 28% F: 72%
Palsa complexes	Palsa complexes are patterned bogs with the presence of palsa hillocks – frost heaves of 0.5-1 height. They arise in the north taiga and prevail northwards. They may include numerous shallow pools.	WH: 12% OH: 37% P: 51%
<i>Open wetlands</i>		
Open bogs	Open bogs are widespread at the periphery of wetland systems. They are characterized by presence of dwarf shrubs-sphagnum hummocks up to 30 cm in height and 50-200 cm in size.	OH: 100%
Open fens	Open fens are the integral class that encompasses all varieties of open rich and poor fens in WSL taiga. They occupy areas with higher mineral supplies at the periphery of wetland systems and along watercourses. The vegetation cover is highly productive and includes sedges, herbs, hypnum and brown mosses.	F: 100%
<i>Water bodies</i>		
Lakes and rivers	All water bodies larger than 60×60 m ² , so they can be directly distinguished by Landsat images.	W: 100%

4

5

1 Table 3. Latitudinal distribution of wetland ecosystem types

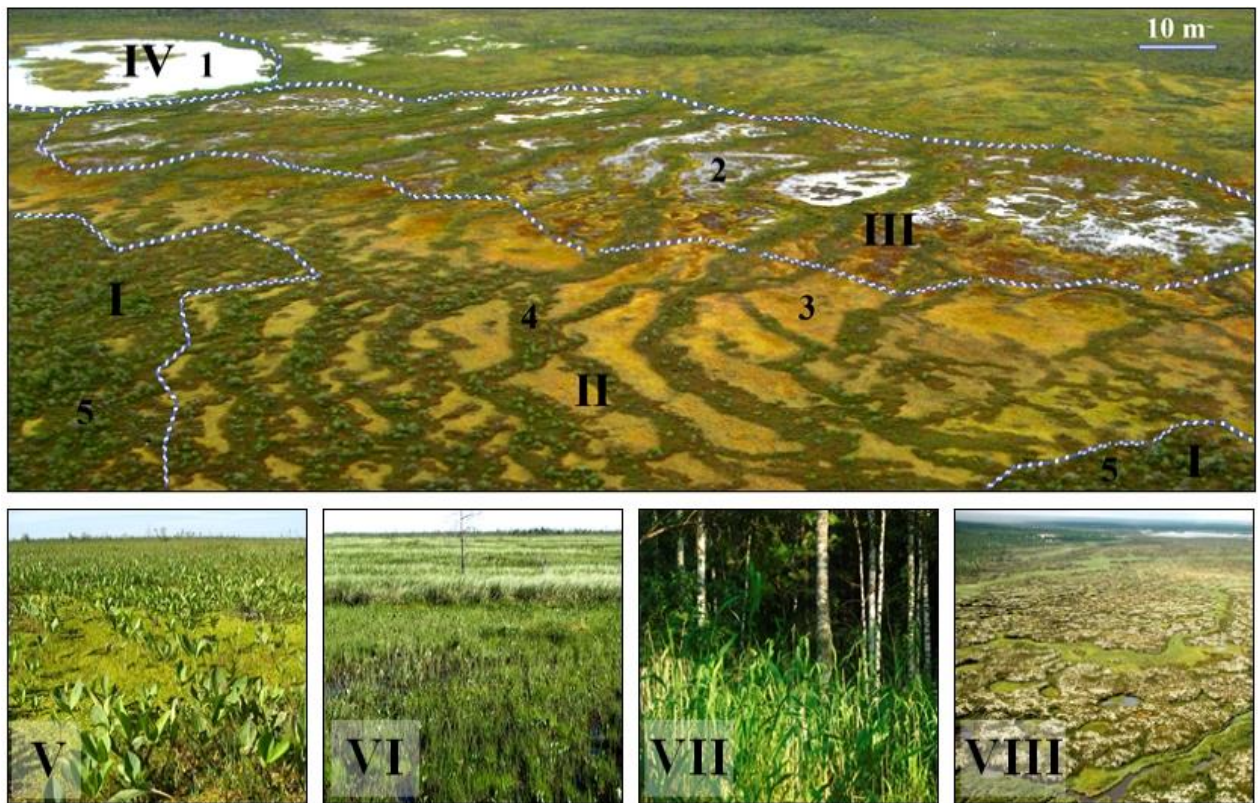
Wetland ecosystem types	South taiga		Middle taiga		North taiga		<i>Total area</i>	
	Area, Mha	%	Area, Mha	%	Area, Mha	%	Area, Mha	%
Open water	0.37	3	1.66	9	3.91	19	5.94	11.3
Waterlogged hollows	0.50	4	1.32	7	3.40	16	5.22	10.0
Oligotrophic hollows	1.87	16	5.78	30	5.60	27	13.25	25.3
Ridges	1.70	14	3.61	19	3.37	16	8.69	16.6
Ryams	3.37	28	5.14	27	1.60	8	10.11	19.3
Fens	4.22	35	1.77	9	1.53	7	7.52	14.3
Palsa hillocks	0.00	0	0.00	0	1.71	8	1.71	3.3
<i>Total wetland area</i>	<i>12.04</i>		<i>19.27</i>		<i>21.13</i>		<i>52.44</i>	
<i>Total zonal area</i>	<i>42.96</i>		<i>56.56</i>		<i>58.46</i>		<i>157.97</i>	
<i>Paludification, %</i>	<i>28.0</i>		<i>34.1</i>		<i>36.1</i>		<i>33.2</i>	

2

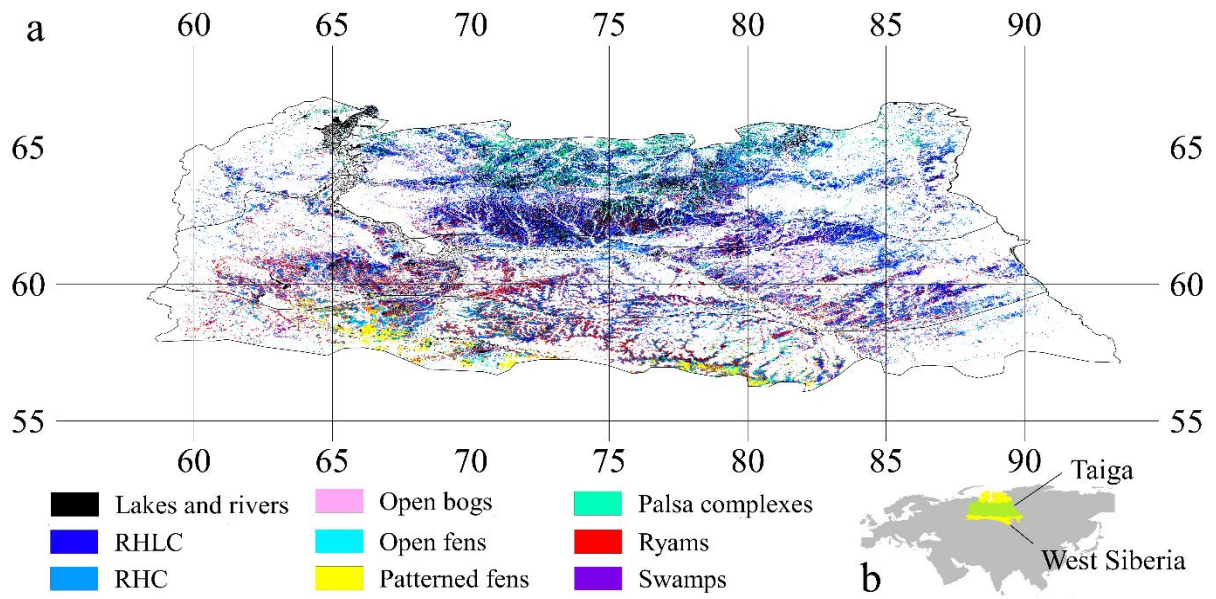
1 Table 4. Confusion matrix of West Siberian wetland map validation (additional 11 floodplain
 2 and 33 mixed class polygons classified as wetlands are not presented)

Real classes Estimated classes	Non-wetland	Lakes and rivers	RHLC	Pine bogs	RHC	Open Fens	Patterned Fens	Swamps	Palsa complexes	Open bogs	Total	UA ¹ , %
Non-wetland	110			1						2	113	97
Lakes and rivers		94	3					1			98	96
RHLC	4	7	69	1	4				2		87	79
Pine bogs	3		1	108	7		4			7	130	83
RHC	1		6	2	150	5	9			8	181	83
Open Fens			3	1	3	86	20			3	116	74
Patterned Fens												
Swamps	1		4	1		18	68				92	74
Palsa complexes	5					4	9	82			100	82
Open bogs	13		1	2	1				54	3	74	73
Total				1	7	1				38	47	81
<i>Total</i>	<i>137</i>	<i>101</i>	<i>87</i>	<i>117</i>	<i>172</i>	<i>114</i>	<i>110</i>	<i>83</i>	<i>56</i>	<i>61</i>	1038	
<i>PA², %</i>	<i>80</i>	<i>93</i>	<i>79</i>	<i>92</i>	<i>87</i>	<i>75</i>	<i>62</i>	<i>99</i>	<i>96</i>	<i>62</i>		

3

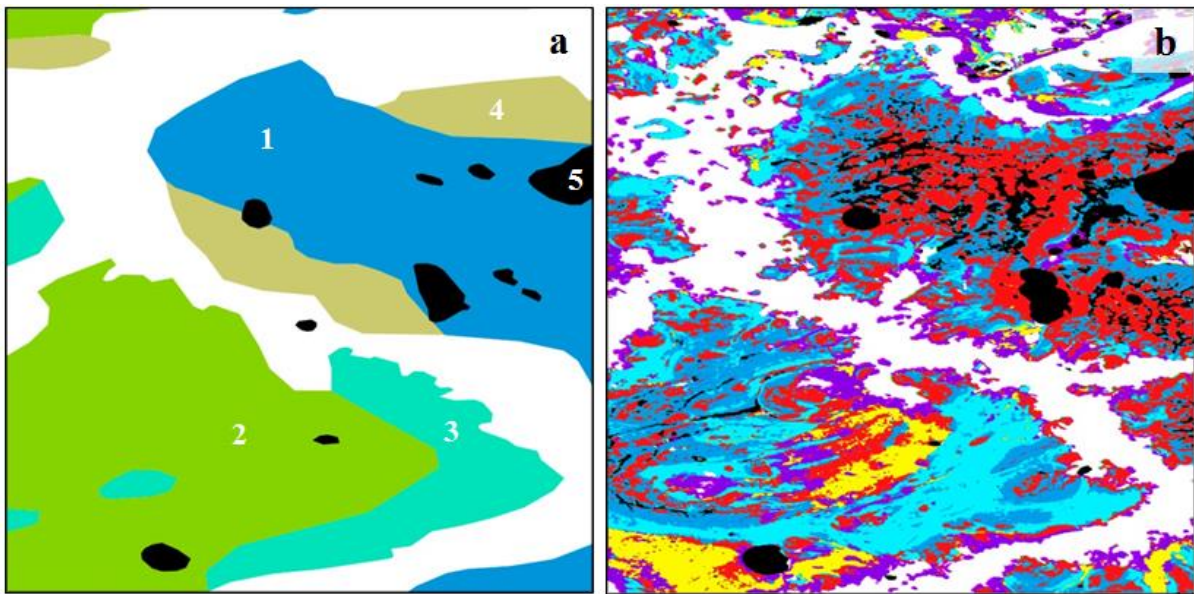


1
 2 Figure 1. Wetland complexes (I – Pine bog or ryam, II – Ridge-hollow complex or RHC, III –
 3 Ridge-hollow-lake complex or RHLC, IV – Lakes and rivers, V – Open fens, VI – Patterned
 4 fens, VII – Swamps, VIII – Palsa complexes) and ecosystems in WSL (1 – Open water, 2 –
 5 Waterlogged hollows, 3 – Oligotrophic hollows, 4 – Ridges, 5 – Ryam)

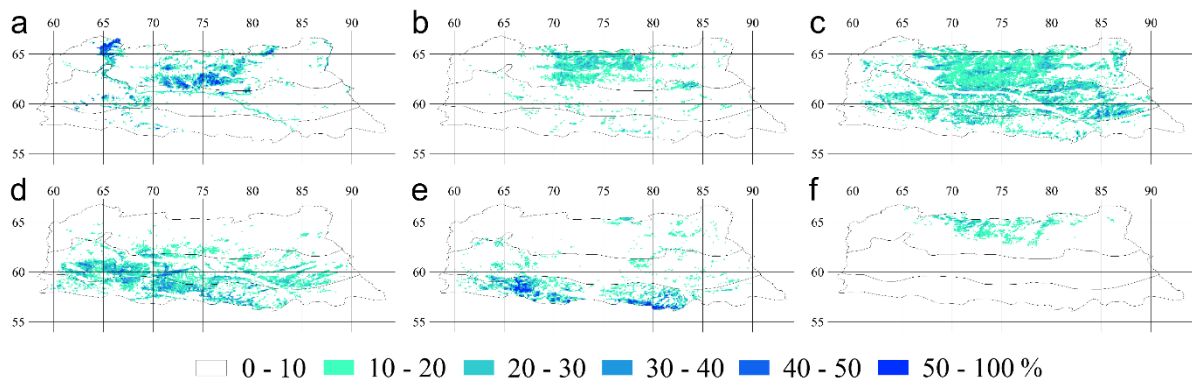


1

2 Figure 2. Wetland map (a) of the WSL taiga zone (b; yellow – WS, green – taiga zone)



1
 2 Figure 3. Comparison of wetland classifications: a – SHI map (1 – Sphagnum-dominated bogs
 3 with pools and open stand of trees, 2 – ridge-hollow, ridge-hollow-pool and ridge-pool
 4 patterned bogs, 3 – forested shrubs- and moss-dominated mires, 4 – moss-dominated treed
 5 mires, 5 – water bodies), b – this study (legend is on Figure 2); 59-59.5°N, 66-66.5°E



2 Figure 4. Wetland ecosystem areas for $0.1^\circ \times 0.1^\circ$ (% from the total cell area): a – open water, b
 3 – waterlogged hollows, c – oligotrophic hollows, d – ryams, e – fens, f – palsas hillocks; the
 4 distribution of ridges is not represented because it is quite similar to the oligotrophic hollow
 5 distribution; the black outlines divide the taiga into the north, middle and south taiga subzones
 6